Modeling of Andean Backarc (30º-36ºS) Crustal Earthquake Waveforms Using a Portable Regional Broadband Seismic Network

PATRICIA ALVARADO[1,2], SUSAN BECK[2], GEORGE ZANDT[2], MARIO ARAUJO[1,3], ENRIQUE TRIEP[4] and THE CHARGE EXPERIMENT GROUP[*]

(1) Departamento de Geofísica y Astronomía – Facultad de Ciencias Exactas, Físicas y Naturales - Universidad Nacional de San Juan. Meglioli 1160 S (5400) Rivadavia, San Juan, Argentina.
e-mail: palvarad@unsj.edu.ar

(2) Department of Geosciences - University of Arizona. Gould Simpson Bldg. 1040 E Fourth St. Tucson, Arizona 85721-0077 USA.
alvarado@geo.arizona.edu beck@geo.arizona.edu zandt@geo.arizona.edu

(3) Instituto Nacional de Prevención Sísmica (INPRES). Roger Ballet 47 N (5400) San Juan, Argentina. e-mail: maraujo@inpres.gov.ar

(4) Instituto Geofísico Sismológico Ing. Fernando Séptimo Volponi - Facultad de Ciencias Exactas, Físicas y Naturales - Universidad Nacional de San Juan. Ruta Provincial Nº 14, Km 17 (5400) Rivadavia, San Juan, Argentina. e-mail: triep@andes.unsj.edu.ar

Abstract. The Nazca and South American plate convergence generates significant crustal earthquakes in the Andean backarc in the vicinity of 30ºS. Moderate to large earthquakes (magnitude ≥7.0) have occurred in Argentina, causing many deaths and much destruction near

San Juan and Mendoza (1861, 1894, 1944, 1952, and 1977). In order to understand the seismotectonic processes in the region, it is important to characterize as many crustal earthquakes as possible. Previous workers determined focal mechanisms for moderate-to-large continental earthquakes modeling seismic waves at teleseismic distances, and using first-motion P-waves. The CHilean ARgentinean Geophysical Experiment (CHARGE) deployed 22 IRIS-PASSCAL broadband seismic instruments across the Andes between 30º-36ºS that operated continuously for 1.5 years (2000-2002). We have used broadband waveforms recorded by CHARGE to determine focal mechanisms of Andean backarc crustal earthquakes. We used a least-squares moment tensor inversion technique, which consists of modeling complete seismic displacement records of moderate-size earthquakes using a seismic structure previously determined. Comparing the synthetic seismograms with observed data we obtained the best double-couple focal mechanism solutions and estimates of the best depths. Our results for three earthquakes ($4.7 \leq m_b \leq 5.3$) that occurred near San Juan (14 December 2001), south of Mendoza (15 March 2001), and near Córdoba (15 March 2002) indicate thrust faulting at shallow and mid-crustal depths (21, 3 and 21 km, respectively).

Resumen. La convergencia entre las placas de Nazca y Sudamericana genera importantes sismos corticales en la región andina de tras-arco alrededor de 30ºS. Por esta razón, terremotos de moderada o gran magnitud (M ≥7.0) han ocurrido en Argentina causando numerosas víctimas y provocando gran destrución en las provincias de San Juan y Mendoza (1861, 1894, 1944, 1952, and 1977). Con el objeto de entender los procesos sismotectónicos en la región, es importante caracterizar la mayor cantidad posible de sismos corticales. Previamente, algunos autores determinaron mecanismos focales para sismos continentales de la region de magnitud moderada-a-grande modelando ondas a distancias telesísmicas y también, utilizando el primer movimiento de ondas P. El Experimento Geofísico Argentino Chileno CHARGE desplegó una red de 22 sismógrafos de banda ancha (IRIS-PASSCAL) a través de los Andes entre 30º-36ºS que operaron en modo continuo durante un año y medio (2000-2002). Utilizando formas de ondas sísmicas de banda ancha registradas por las estaciones sismológicas del CHARGE y una estructura de velocidades previamente determinada, hemos obtenido mecanismos focales para sismos corticales de magnitud moderada ocurridos en la región andina de tras-arco. La técnica empleada invierte el tensor de momento sísmico modelando las tres componentes de los desplazamientos sísmicos para ondas de cuerpo y superficiales utilizando un ajuste por mínimos cuadrados y una estructura sísmica conocida. La comparación entre los sismogramas sintéticos y observados permite obtener la solución más probable correspondiente a un mecanismo focal de doble-cupla y también estimar la “mejor” profundidad focal. Nuestros resultados para tres sismos ($4.7 \leq m_b \leq 5.3$) que ocurrieron en San Juan (14 de diciembre de 2001), sur de Mendoza (15 de marzo de 2001) y norte de Córdoba (15 de marzo de 2002), indican fallamiento de tipo inverso para profundidades superficiales y de corteza media (21, 3 y 21 km, respectivamente).

INTRODUCTION

The subduction of the Nazca plate beneath South America at a relative plate motion of ~8.5 cm/yr (DeMets et al., 1990) generates east-west compression along the western edge of South America. Between 30º and 36ºS, large numbers of earthquakes occur in the west-central part of Argentina. In particular, two different depths of seismicity exist in the backarc of the Andes, which overrides a flat subducting slab (north of ~33ºS). Earthquake hypocenters indicate a deep zone at about 100-200 km in depth (Fig. 1) corresponding to the Nazca slab (Cahill and Isacks, 1992). Seismicity is also observed in the crust and is mainly related with the uplift of the Precordillera and Pampean ranges (Fig. 2). Occasional large, shallow intraplate earthquakes (depth <50 km) have caused many deaths and much destruction. The 1861 earthquake (M=7.0) destroyed the city of Mendoza, killing ~7,000 people, approximately one third of the city's population at that time (Zamarbide and Castano, 1993). In the last century, three more strong earthquakes of magnitudes M_s=7.4, 7.0 and 7.4 with depths less than 30 km occurred in 1944, 1952 and 1977, respectively. For that century, the 1944 earthquake was the most destructive in the Argentinean history, causing 10,000 deaths in a population of 90,000 and devastating 80% of the city in the epicentral area around San Juan (INPRES, 2003). Damage has been estimated at 100 million dollars at the time of this event (Ganse and Nelson, 1981). This shallow intracontinental seismicity extends as far as 600 km to the east of the high peaks of the Andes. Córdoba and San Luis have been the sites of damaging earthquakes with magnitudes 6.0 and 6.4 in 1934 and 1936, respectively.

The largest events that have occurred in the region since 1963 have been studied using the global seismic network. Moderate-to-large earthquakes are well recorded at teleseismic distances (Fig. 3a), but small-to-moderate earthquakes, barely recorded at these distances, are more abundant, and their analysis is important to understanding the active tectonics of a region. Permanent short-period seismic networks had a tremendous impact in improving detection, location, and often first-motion focal mechanism determinations (Fig. 3b and Table 1). Thus, in the last 20 years, the Argentinean and Chilean permanent seismic networks reported 489 earthquakes (depth <50 km) located in the Andean cordillera and backarc region with magnitudes greater than 4.0. Only 6.5% of those earthquakes had magnitudes M >5.0 (Fig. 3b). Digital broadband portable regional seismic arrays are very useful in providing digital records of small-to-large earthquakes that are not well recorded by the global networks.

In this work, we summarize the backarc crustal seismicity and present the seismic moment tensor inversion for three earthquakes that occurred to the east of the Andes recorded on temporary broadband seismic stations.

The CHilean ARgentinean Geophysical Experiment (CHARGE) was an international project that involved researchers and students of the University of Arizona (USA), the National University of San Juan (Argentina), the National Institute of Seismic Mitigation (INPRES, San Juan, Argentina), and the University of Chile (Chile). The CHARGE experiment deployed 22 IRIS-PASSCAL broadband seismic instruments across the Andes between 30º-36ºS that operated continuously for 1.5 years (2000-2002) (Fig. 1). In this time period, the network recorded four shallow events (depth <50 km) of magnitudes M >5.0 and 71 events of magnitude $4.0 \leq M \leq 5.0$ located in the Andean cordillera and backarc region (Fig. 3c). By modeling regional waveform data we constrained the focal mechanism solutions and depths for two of the largest crustal events (M_D=5.0 and m_b=5.3) that occurred in Argentina in 2001 within the CHARGE network. In addition, one smaller crustal earthquake (m_b=4.7) that occurred in the easternmost part of the region in 2002 was also analyzed. We refer to these earthquakes herein by their corresponding year and Julian day (e.g., 14 December 2001 is 01348). Figure 3c shows the relative size and epicentral locations of events 01074, 01348 and 02074 studied here, which are associated with different geological provinces of Argentina (Fig. 2). The tectonic implications of the results are interpreted within a seismic framework determined from previous studies in the region. In addition, our estimates for hypocentral depths are compared with global earthquake location information. The preliminary determination of epicenters (PDE) catalog from the National Earthquake Information Center (NEIC, USA) located the events that we modeled at a depth of 33 km, but this is a “fixed” value when global waveforms cannot resolve the depth. Thus, the regional moment tensor inversions provide another technique to determine and discuss focal depths.

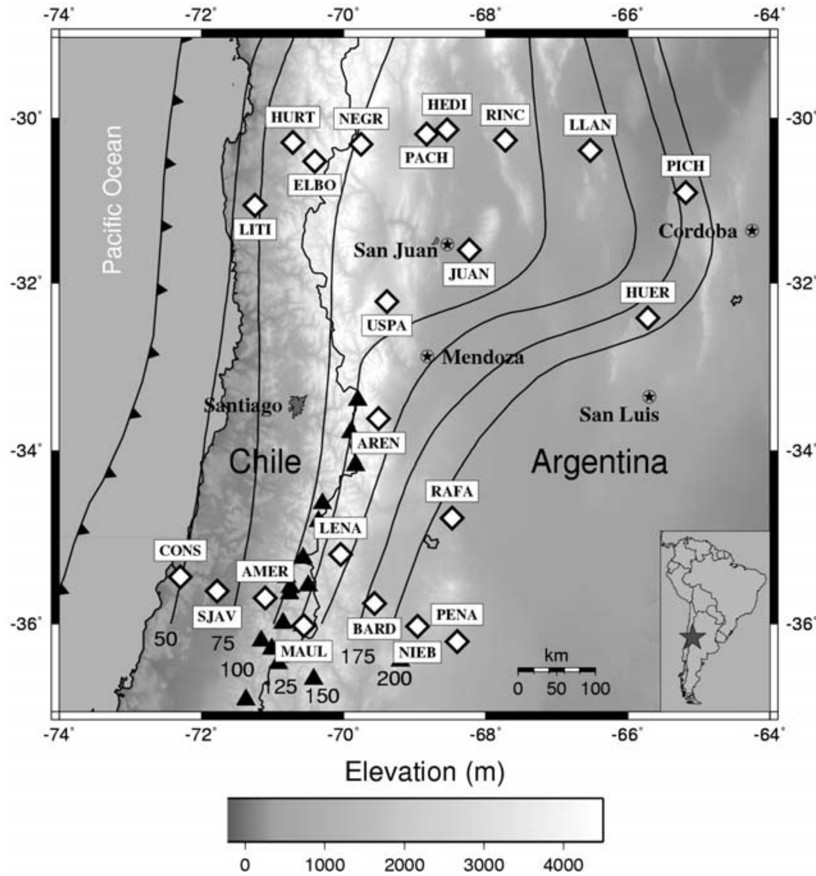

Fig. 1. Map of the south-central Andes showing the location of the CHilean Argentinean Geophysical Experiment (CHARGE) portable broadband seismic instruments (diamonds) from IRIS-PASSCAL (USA); one station (AREN) from UNSJ (Argentina); and one station (RAFA) from INPRES (Argentina). The seismic network operated continuously from November 2000 to May 2002. Saw-toothed line marks the axis of the trench where the Nazca and South American plates converge at ~8.5 cm/yr (DeMets et al., 1990). The contours are the depth in kilometers to the subducted Nazca slab (Cahill and Isacks, 1992). Black triangles show the location of the active volcanoes. Note the correlation between flat subduction and lack of active volcanism.

REGIONAL GEOLOGIC AND TECTONIC SETTING

The topography of the Andes (Fig. 1) was built as a result of the compression produced by the interaction between the Nazca and South American plates. For the region of study, the main cordillera exhibits the highest elevations with peaks over 6000 m along a narrow N-S chain (Figs. 1 and 2). The Tupungatito volcano (33.4ºS, 69.8ºW) represents the beginning of an active volcanic arc south of 33ºS latitude, which coincides with the resumption of a normal subduction geometry of a dip angle of ~30º. In contrast, north of 33ºS, volcanism shut off ~10Ma ago (Kay et al., 1988; Kay and Mpodozis, 2002). Some authors correlate this event with the progressive flattening of the Wadati-Benioff zone in that segment, which also produced an eastward migration of volcanism beginning in the Early Miocene (Kay et al., 1988; Ramos et al., 1991). The subducting Juan Fernández Ridge on the Nazca Plate is mentioned as a major bathymetric feature controling flat subduction (Gutscher et al., 2000; Yañez et al., 2002). The tectonic style of the main Cordillera is also different in the northern and southern segments. Shortening rates are absorbed by the Precordillera fold and thrust belt in the north part (Cristallini and Ramos, 2000). Although considerably less shortened, the main Cordillera between 34º and 38ºS is also under contraction by development of a fold and thrust belt (Ramos, 1988, 1989).

Overriding the flat subduction segment, the Precordillera encompasses the foothills of the Andes (Fig. 2). This thrust belt, composed of Paleozoic clastics, is deformed with a thin-skinned style (Baldis et al., 1982), although thick-skinned deformation and vergence orientation changes have been observed in its eastern part (Allmendinger et al., 1990; Zapata and Allmendinger, 1996). Crustal seismic activity related to the Precordillera increases to the east (Smalley et al., 1993).

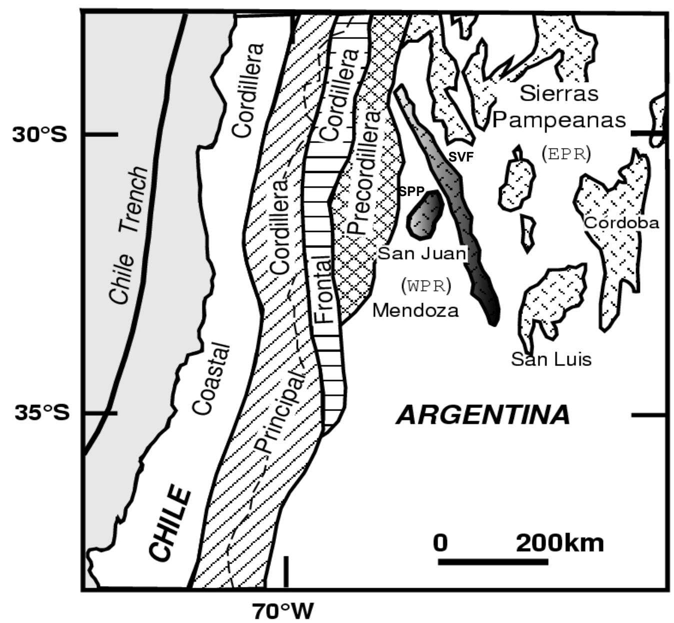

Fig. 2. Geological provinces of the central Andes (modified from Ramos et al., 1996). In the eastern foreland region, basement block uplifts of the Sierras Pampeanas are shaded light for the Eastern Pampean Ranges (EPR) and dark for the Western Pampean Ranges (WPR). The oval-shaped range in the WPR is Sierra de Pie de Palo (SPP), where the 1977 San Juan earthquake took place; the other dark elongated system is Sierra de Valle Fértil-La Huerta (SVF).

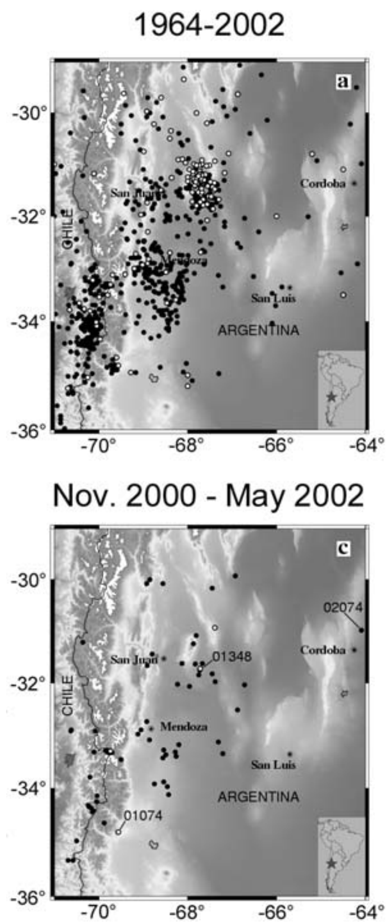

Fig. 3. PDE locations of shallow events (depth <50 km) that occurred (a) in the last ~40 years, (b) in the last 20 years, and (c) during the CHARGE experiment. White and black circles are events with magnitudes >5.0 and between 4.0-5.0, respectively. Compare the seismicity that occurred in the different data intervals and note how after 1982 permanent seismic networks of both countries have helped to detect small-to-moderate sized earthquakes. San Juan and Mendoza are the most seismically hazardous cities of Argentina. The crustal seismicity is less abundant to the east. The Pie de Palo range (Fig. 2) has the largest concentration of recent larger events. The intense seismic activity observed in map (a) beneath this geologic structure is mainly related to the 1977 Caucete, San Juan earthquake (Figs. 4 and 5). Also shown in (c) are the earthquakes in this study referred to by their corresponding year and Julian day.

In the eastward foreland region, Precambrian metamorphic crystalline rocks of thick-skinned deformation are building basement uplifted blocks of the Sierras Pampeanas (Fig. 2). Although they are not part of the cordillera as it is defined, their deformation style is a response to the Andean orogeny (Jordan and Allmendinger, 1986). Generally, north-south striking thrust or reverse faults bound the ranges, which are separated by broad intervening valleys. The Sierra Pie de Palo (San Juan), composed of rocks as old as 1.1 Ga (McDonough et al., 1993), is probably the most seismically active mountain block of the Sierras Pampeanas; it has been the site of the last large earthquake (M_s=7.4) that occurred in the area (Caucete-San Juan, 1977). Basic and ultrabasic rocks are more common in the Western Pampean Ranges, with scarce granitic bodies. These granites, however, characterize the Eastern Pampean Ranges, sometimes reaching batholithic dimensions (Caminos, 1979). Ages for volcanic centers related to subduction magmas in this eastern part are ~4.7-7.9 Ma (Gordillo and Linares, 1981; Kay and Gordillo, 1994). The youngest magmatic activity recorded in the Sierras Pampeanas comes from the Sierra El Morro (San Luis), indicating that such activity ended ~1.9 Ma (Ramos et al., 2002).

PREVIOUS FOCAL MECHANISM DETERMINATIONS

Seismic phase information, leveling surveys, and direct observations have been used in the past decades to estimate the movements along the fault planes that caused the 1861, 1894, 1936, 1944, 1964, and 1977 earthquakes (Groeber, 1944; Castellanos, 1944; Volponi et al., 1966; Bastías et al., 1984; Kadinsky-Cade et al., 1985; Langer and Bollinger, 1988; Costa and Vita-Finzi, 1996; Perucca and Paredes, 2003). The locations and magnitudes of the earthquakes that have occurred in the region since 1782 are shown in Figure 4.

P wave first motions and S wave polarization angles were used to determine the focal mechanism of an event (m_b=5.9) that occurred near Valle Fértil range in 1965 (Stauder, 1973). Seismicity located at shallow depths under the Sierra Pie de Palo, which is mainly related to the 1977 (M_s=7.4) earthquake, has also been studied using P wave first motions (Algermissen et al., 1978; Volponi, 1979; Triep and

Cardinali, 1984). Other data from a PANDA short-period passive seismic experiment carried out around San Juan (1987-1988) was analyzed with this technique, resulting in 120 focal mechanisms in the basement uplift region (Regnier et al., 1992). The 1985 earthquake, which occurred within the area of the Barrancas anticline close to Mendoza, was also studied using this technique and the aftershock distribution (INPRES, 1985; Triep and Quiroga, 1989; Assumpção, 1992; Chiaramonte et al., 2000).

Chinn and Isacks (1983) used long-period P waveforms to determine the focal mechanisms and to estimate the depths (error less than 5km) for the 1963, 1965, 1972 and 1977 earthquakes. This method has the advantage of being less affected by the complexities of the crustal structure and the source process, but it is highly dependent on the delay between the direct P and surface reflected phases and hence the depth. Assumpção and Araujo (1993) determined the focal mechanisms for three earthquakes that occurred in 1967, 1977 and 1979 by inversion of teleseismic body waves (short-period P waves and long-period SH waves) using the method developed by Nábelek (1984). Using very long period waveforms (T >40 s) from the global network, earthquakes of magnitude $M_s \geq 5.5$ were analyzed using the centroid moment tensor (CMT) method (Dziewonski et al., 1981). This information (available since 1976) includes the focal mechanisms and other parameters for 19 shallow earthquakes that occurred in the region. The Harvard-CMT catalog contains the 1977 and 1985 earthquakes as well as the most important aftershocks of the former event. Similar seismic modeling techniques were used to study these bigger events utilizing surface waves (Triep, 1979, 1987) and diffracted P-waves (Kadinsky-Cade, 1985).

Table 1 and Figures 4 and 5 summarize the available information for 98 earthquakes that occurred in the last ~40 years. The cited authors obtained the first 95 earthquake estimations. Previous parameters are very useful in providing a tectonic characterization of the region. We will use this summary to compare with our results, refering to earthquakes in Table 1 by their corresponding numbers. From this summary, it is clear that no extensional faulting with moderate to large magnitudes has yet been clearly identified in the crustal backarc of Argentina. Predominant thrust and some strike-slip focal mechanisms have an average orientation for the maximum compressive P axis of azimuth 88º and plunge ~9º with an extensional T-axis near vertical. This observation is only based on modeled seismic data and it is 9 degrees more clockwise than the plate convergence direction N77º±12ºE (DeMets et al., 1990). The smallest earthquake analyzed using seismic modeling methods occurred on 24 December 1979 with magnitude m_b=5.3; M_s=4.6; and M_w=5.0 (event 49 from Assumpção and Araujo, 1993). No determinations exist for the Eastern Pampean Ranges. In contrast, a larger number of earthquakes have occurred in the vicinity of the Sierra Pie de Palo; thirty-eight of them are probably related to the 1977 Caucete, San Juan earthquake. The region near Mendoza city was the site of the 1985 (M_w=5.9) earthquake. Focal mechanism, geologic and seismic reflection information demonstrated that new faults located deeper than the east Barrancas anticline fault were responsible for this event (Chiaramonte et al., 2000). The 1967 earthquake m_b=5.4 (event 4) that occurred in this area had a thrust focal mechanism solution. Two moderate events (numbers 50 and 94) separated by 20 years have occurred west around this latitude. Also, one earthquake m_b=5.4 (event 7) that occurred in 1977 was located to the south. All of these events have focal mechanisms with a large component of strike-slip motion. In the southernmost study area, only one moderate seismic event (M_w=5.9) occurred in 1999 (event 93). Its Harvard-CMT solution will be discussed latter in view of its close proximity to the event 01074 studied here. Finally, three earthquakes located in the north part of the region correspond to the 1963 (event 1), 1965 (event 3), and 1979 (event 49) earthquakes. The location of the 1963 seismic event is very close to the epicenter of the 1894 earthquake (Fig. 4), which is probably the largest event in the region (M≅8). The 1963 event focal mechanism solution indicates thrust faulting. The focal mechanism and hypocentral depth of the 1965 earthquake together with seismic reflection studies indicate that it is likely related to the Valle Fértil thrust fault associated with the uplift of the range of the same name (Snyder et al., 1990; Zapata, 1998).

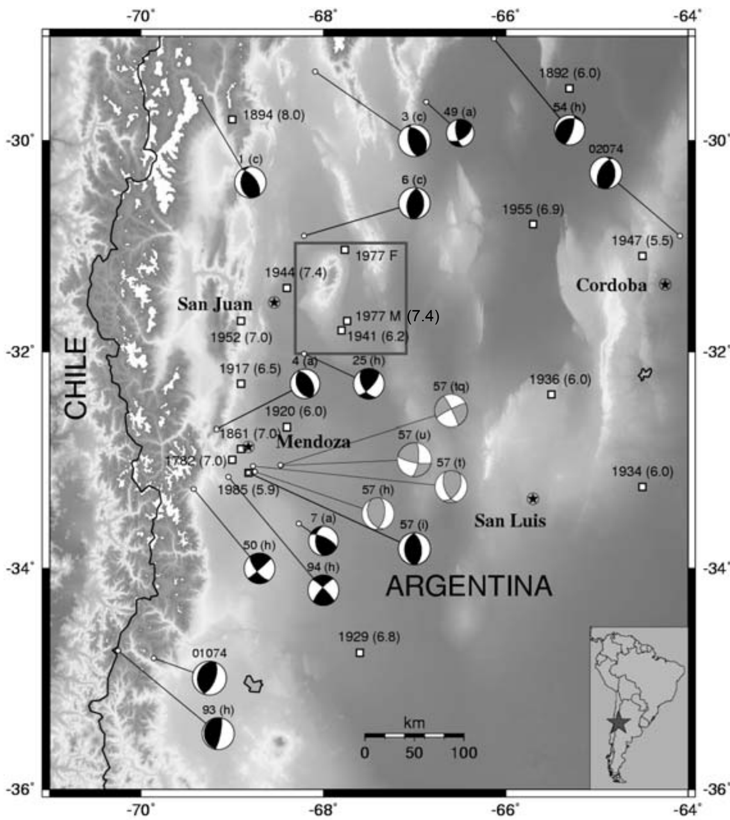

Fig. 4. Epicenters of the damaging historical earthquakes that occurred in the region (dated squares with magnitudes in parentheses). Also shown are lower-hemisphere focal mechanisms determined from synthetic modeling by others seismic studies referred to in the text and Table 1. Dark quadrants indicate compressive first motions. Gray colors are used for different solutions of the 1985 Mendoza earthquake (event 57). The solutions for events 01074 and 02074 were obtained in this study through the moment tensor inversion using regional broadband seismic waveforms recorded on the CHARGE network. Location of map of Fig. 5 containing the other event in this study (01348) is indicated by the larger square with the dark gray boundary. (See text and Table 1 for references.)

Table 1. Parameters of intraplate earthquakes of the Andean backarc between 29º-36ºS and 64º-71ºW.

Earthquake Number	Date yr/m/d	Origin Time hr/m	Latitude South	Longitude West	Depth (km)	Focal Mechanism Parameters					Seismic Moment 10^{25}dyn cm	M_s	m_b	M_w	Reference
						Nodal Planes			P axis						
						Strike	Dip	Slip	Azimuth	Plunge					
1	630518	0533	29.59	69.35	41	180	38	120	69	11		5.7			(c)
						324	58	69							
2	641118	0501	31.2	67.6	8	39.3	76	20.2	89.2	10.5			5.5		(tc)
						304.7	70	166							
3	651113	1759	29.3	68.1	34	170	58	106	248	12			5.9		(s)
						321	36	65							
			29.34	68.09	32	321	36	66	248	11	0.41	6.0	5.9		(c)
						170	57	107							
			29.3	68.1	34	62.2	70	67.4	81.5	21.2			6.0		(tc)
						294.6	30	136.3							
4	670425	1036	32.72	69.17	27	159	41	97	64	4	0.17	4.7	5.4	5.4	(a)
						330	49	84							
5	681024	1734	30.304	68.236	38	60.6	74	42	94.5	15.4					(tc)
						316.8	50	159							
6	720926	2105	30.91	68.21	20	192	51	98	277	6	1.20	6.0	5.8		(c)
						360	40	80							
			30.913	68.102	16	52	66	31.6	91.4	5					(tc)
						307.7	61	152							
7	770125	0050	33.59	68.27	18	180	45	147	53	13	0.12	5.0	5.4	5.3	(a)
						295	67	50							
8	771123	0926	31.1	67.7	<30	340	79	151	~34	~11		7.1			(ac)
						~70	~59	~12							
			31.041	67.764	17	313	70	77	54	66		7.4			(v)
						165	25	119							
			31.088	67.854	13	325.6	70	47.6	84.7	14		7.4	6.3		(tc)
						305.6	46	152.3							
			31.028	67.767	13.2	350	80	73	94	33	300	7.4	6.3		(t *-1979*)
						230	20	149							
			31.04	67.76	17	166	40	90	76	5	34.41	7.3	6.4	7.4	(c)
						346	50	90							

			31.22	67.69	20.8	183	44	90	94	1	186	7.4	6.3		(h)
						4	46	90							
			31.15	67.78	17	166	40	90	76	5	130	7.3			(k)
						346	50	90							
9	771123	1158	31.069	67.961	21	62.5	78	82	68.8	32.3			5.9		(tc)
						272.4	14	119.4							
10	771123	1305	31.149	67.774	27	77.6	70	77.7	87	23.7			5.6		
						289.6	23	120							(tc)
						30.4	78	20	72	5.2					
						295.7	70	167							
11	771123	1636	31.374	67.833	13	292.5	70	164.8	78.7	7.8		5.4	5.7		(tc)
						28.4	75	20.9							
12	771123	2152	31.390	67.651	33	274.3	74	162.8	52.2	0.1			5.4		(tc)
						9.4	73	17							
13	771123	2157	31.758	67.851	33	42.8	79	22.7	84.4	7.6			5.1		(tc)
						308.2	67	168							
						80.6	71	90	80.7	26					
						260.6	19	90							
14	771123	2327	31.660	67.761	33	40	80	23	81.5	8.6		4.8	5.5		(tc)
						306	67	169.5							
15	771124	0157	31.609	67.774	33	26	84	15	69.6	6		5.8	5.6		(tc)
						294.3	75	174							
						54.4	77	92	50	32					
						223	13	81.3							
16	771124	0202	31.618	67.854	23	22.1	70	32	59.3	6.2		6.3	5.7		(tc)
						280.3	60	157.6							
17	771124	1820	31.253	67.681	33	28.2	74	20.0	69.6	2			5.7		(tc)
						292.2	70	162.7							
			31.53	68.05	46.5	190	34	91	99	11	0.281		5.7	5.6	(h)
						8	56	89							
18	771124	1842	31.292	67.795	33	57.6	76	80.1	65.8	30.2		4.8	5.7		(tc)
19*	771210	0836	31.253	67.743	33	273.4	17	125							
						57.6	76	99	50.7	30.2					
						204.7	16	58.2							

20	771124	2300	31.207	67.737	33	66.3	80	82.3	73	34.5			5.3		(tc)
						283.1	12	128.7							
						19	90	30	60	21					
						289	60	180							
21	771125	0324	31.644	67.779	33	23.8	84	15	67.1	6			5.1		(tc)
						291.9	75	174							
						81.7	72	109.3	61.4	24.2					
						209	26	45.5							
22	771125	0347	31.698	67.579	33	28.4	84	15	71.7	6			5.0		(tc)
						296.5	75	174							
						64.9	78	84	70	32.5					
						270	13	104.5							
23	771125	0406	31.065	67.806		67.5	74	70.6	83	27			4.9		(tc)
						299	25	138.4							
						28.7	84	6	73.1	0					
						298.1	84	174							
24	771128	0017	31.103	67.760	33	53	78	44	84.8	18.7			5.4		(tc)
						311.2	47	163.4							
25	771128	0419	31.672	67.778	35	23	78	3.7	248.2	5.8		5.4	5.5		(tc)
						291.8	86	168							
						81.6	72	138	48.8	13					
						186.8	50	24							
			32.02	68.21	33.1	150	52	27	100	10	0.284	5.4	5.5	5.6	(h)
						43	69	139							
26	771128	0539	30.922	68.133	9	65	80	118	42.3	29.4		4.9	5.4		(tc)
						172.5	30	20							
27	771128	0631	31.44	67.44	15	170	30	100	72	15	1.41	5.8	5.9		(c)
						338	60	84							
			31.502	67.532	15	64.4	76	47	94.6	18.7		5.8	5.7		(tc)
						319	45	159.5							
			31.67	67.64	15	182	21	106	80	25	2.02	5.8	5.7	6.1	(h)
						345	70	84							
			31.48	67.45	15	170	30	100	72	15		5.8			(k)
						338	60	84							

28	771128	0805	31.573	67.259	33	69.7	75	96	63.1	29.6			4.8		(tc)
						229.5	16	72.4							
29	771205	1543	31.063	68.043	32	293.5	80	176	70	4.5		5.6	5.4		(tc)
						24.5	86	9.6							
						292.4	70	159	71.5	0					
						29.9	70	20.5							
			31.57	68.22	32	103	65	-5	61	21	0.497	5.6	5.4	5.7	(h)
						195	86	-154							
30	771206	0841	31.014	67.820	35	77.6	70	77.7	87	23.7		5.1	5.6		(tc)
						289.6	23	120							
						41	80	19.4	84	7					
						309	70	170							
31	771206	1705	31.24	67.90	18	180	39	62	109	9		5.9	5.9		(c)
						34	56	110							
			31.168	67.718	18	71.6	73	76	86.5	26.5		5.9	5.9		(tc)
						292	22	128.5							
						41	80	19.4	84	7					
						309	70	170							
			31.43	68.11	19	181	37	82	97	8	0.795	5.9	5.9	5.9	(h)
						11	54	96							
			31.24	67.9	25	180	39	62	109	9		5.9			(k)
						34	56	110							
32	771206	1827	31.276	67.843	33	77.6	70	85.7	80.5	25			5.2		(tc)
						267.7	20	100							
						77.6	70	176	211	11					
						168.8	86	20							
33	771207	0322	31.175	67.894	33	314.7	68	80.4	153.7	65			5.2		(tc)
						109.8	24	-113.4							
34	771209	2144	31.618	67.846	37	260	82	-72.7	97.6	50		4.3	5.2		(tc)
						13	18	-151.5							
35	771210	0711	31.187	67.639	38	86.6	78	74	100	32		4.8	5.6		(tc)
						319.3	20	141.6							
			31.28	68.03	34.9	199	29	117	89	18	0.192	4.8	5.6	5.5	(h)
						348	65	76							

36	771210	1419	31.207	67.743	27	260 169.3 26.5 120.2	84 85 78 70	-175 -6.0 -20 -167.3	34.4 252	8 22.5		4.7	5.0		(tc)
37	771213	1006	31.596	67.431	33	27.5 290.6 286 34.3	70 74 64 58	17.5 159 143.7 31.7	64.6 251	6.2 3.4			5.4		(tc)
38	780103	0110	31.551	67.829	40	48.2 277.8 48.2 158.8	81 14 81 24	79.2 139.6 112.9 22.8	57.3 28.8	24.8 32			5.2		(tc)
39	780117	1133	31.331 31.53	67.937 68.08	24 23	45.6 306.8 142 47	76 55 66 79	35.7 162 12 156	82 96	14 8	 1.07	5.7 5.7	5.8 5.8	 6.0	(tc) (h)
40	780124	1318	31.695	68.868	19	66.9 246.9	80 10	85 90	67.1	35			5.7		(tc)
41	780404	1933	31.263	67.829	10	55.6 314.4 105 352.5	78 36 70 44	55 160 48.5 150.5	82.7 133.8	24.5 15		4.4	5.5		(tc)
42	780626	1849	31.573	67.752	10	26.4 119.1	50 86	-5 -150	256.3	24		4.1	5.0		(tc)
43	780726	0147	31.522	67.583	29	73.4 324.7	60 60	35.5 145.5	109.5	0.6			5.0		(tc)
44	780821	0028	31.271 31.79	67.773 68.11	10 25	69.7 36.2 218 49	79 25 9 81	62 154 79 92	94 137	28.8 36	 0.116	4.7 4.7	5.6 5.6	 5.3	(tc) (h)

45	781025	0136	31.525	67.712	46	36.4	66	31	73.9	3		4.3	5.3		(tc)
						293.6	62	153.3							
46	790830	1859	31.381	67.627	32	290.6	71	159.5	69.2	0.2		5.1	5.3		(tc)
						28.2	71	21							
			31.40	67.06	27	354	31	35	303	23	0.203	5.1	5.3	5.5	(h)
						233	73	116							
47	791008	0152	31.366	67.842	14	305.6	68	131	277.8	13			4.8		(tc)
48*	791127	1737	31.376	67.881	10	58.6	46	32							
49	791224	0013	29.63	66.87	27	168	65	41	290	7	0.041	4.6	5.3	5.0	(a)
						58	53	148							
50	800114	2151	33.27	69.42	15	141	69	5	97	11	0.292	5.2	5.6	5.6	(h)
						49	85	159							
51	800117	1100	31.496	67.710	10	295	50	172	66.7	22			4.9		(tc)
						30.5	84	40							
52	800409	0817	31.654	67.476	10	55.2	79	22.7	96.2	7.6		4.3	5.5		(tc)
						320.7	67	168							
			31.49	67.42	15	340	37	136	218	15	0.128	4.3	5.5	5.3	(h)
						108	65	61							
53	801110	1624	31.576	67.468	20	69.7	75	96	63.1	29.6		5.4	5.7		(tc)
						229.5	16	72.4							
						69.7	75	146.9	31.8	10.6					
						169.5	58	17.3							
			31.52	67.55	15	133	31	49	73	20	0.360	5.4	5.7	5.6	(h)
						358	67	111							
54	830402	0558	29.02	66.13	40.1	247	25	137	122	26	0.102	4.9	5.5	5.3	(h)
						17	73	71							
55	850118	1440	31.91	66.79	22	112.42	45.79	-50.57	96.743	62.197					(tq)
						242.72	56.38	-123.14							
56	850126	0306	33.12	68.57	5	9.46	9.29	-105.93	118.708	53.86					(tq)
						205.62	81.07	-87.43							
57	850126	0307	33.053	68.467	10	7	71	166	233	5	2.0			6.2	(u)
						102	77	20							
			33.12	68.82	12	185.53	40.16	9891	89.21	5.16		5.4	5.9		(i)
						353.94	50.31	82.55							
			33.06	68.77	14	30	46.9	129.4	272	6	0.5			5.7	(t -*1987*)

			33.05 33.11	68.47 68.75	5 28.4	160 242.86 333.59 158 9	56 82.65 84.34 38 56	56 -5.7 -172.62 65 108	198.322 86	9.216 9	1.02	5.8	6.0 6.1	5.9	(tq) (h)
58	850126	0357	33.07	68.47	5	255.38 135.9	40.91 66.9	36.8 124.76	14.893	201.245			5.2		(tq)
59	850126	0625	33.09	68.58	5	251.4 73.45	29.01 61.01	88.21 90.99	162.716	16.002			4.4		(tq)
60	850126	2341	33.15	68.57	5	54.51 225.92	85.37 4.68	-89.3 -98.56	325.272	49.621					(tq)
61	850128	0810	33.10	68.57	5	114.71 282.63	40.03 50.6	80.7 -97.73	149.543	81.994					(tq)
62	850202	0950	31.58	67.81	20	306.30 58.57	7.13 87.28	157.56 83.4	154.844	41.922					(tq)
63	850206	0119	33.06	68.60	5	106.02 255.34	21.15 71.6	118.96 79.39	353.662	25.865					(tq)
64	850207	1332	33.07	68.59	5	340.82 74.96	11.7 89.14	175.77 78.33	176.24	42.987					(tq)
65	850210	0254	33.09	68.48	5	118.20 223.26	89.13 3.36	-86.76 -164.91	31.481	45.78					(tq)
66	850210	0258	33.09	68.53	5	246.81 100	23.11 70.35	58.96 102.41	180.4	24.366			3.6		(tq)
67	850210	1537	34.68	69.78	33	254.15 145.76	13.95 85.52	-161.09 -76.78	69.711	47.86					(tq)
68	850211	1502	33.10	68.45	0	230.03 346.25	10.74 85.21	153.37 80.37	85.066	39.467					(tq)
69	850213	1255	33.11	68.53	5	189.6 81.34	75.58 39.39	52.94 156.89	306.902	21.741					(tq)
70	850302	0202	31.63	68.73	10	264.24 1.9	85.12 32.64	122.31 9.08	327.662	32.365					(tq)
71	850311	1130	33.33	68.18	44.7	139.56 319.61	46.83 43.17	-90.03 -89.97	48.869	88.174			4.7		(tq)
72	850311	1501	33.27	68.18	5	240.03 144.21	26.28 87.13	-173.51 -63.87	78.997	42.022					(tq)
73	850315	1354	31.83	67.04	10	225.58	67.67	-158.89	85.771	30.281					(tq)

						127.23	70.54	-23.77							
74	850327	0757	32.17	69.23	33	173.33 299.42	38.92 64.56	-43.14 -120.51	165.817	58.639					(tq)
75	850406	0854	33.64	68.74	5	267.37 157.16	11.82 85.86	20.61 101.08	236.961	39.875					(tq)
76	850425	1105	33.05	68.61	10	130.05 37.77	0.52 89.98	2.29 90.52	127.247	44.977					(tq)
77	850502	0040	32.13	69.11	33	248.27 72.61	47.94 42.15	87.09 93.22	340.329	2.896					(tq)
78	850502	1932	33.56	68.73	33	333.98 133.9	49.62 42.16	103.32 74.84	54.582	3.787					(tq)
79	850506	1926	31.25	67.84	10	257.13 49.44	27.73 65.04	-65.09 -102.49	295.826	67.564					(tq)
80	850518	0211	28.84	68.37	33	86.44 280.88	7.71 82.53	-104.32 -88.08	193.109	52.435					(tq)
81	850522	0501	26.55	64.71	41	8.19 201.25	45.33 45.42	-99.26 -80.75	194.310	83.428			4.7		(tq)
82	850607	2153	30.38	67.74	16	307.91 130.31	40.74 49.29	88.18 91.56	219.196	4.278					(tq)
83	850615	1256	33.05	68.82	23	218.6 311.76	70.97 80.93	9170.4 19.28	84	6.834					(tq)
84	850701	1036	31.14	67.79	10	219.83 69.11	45.92 47.99	68.69 110.57	144.725	1.071					(tq)
85	850707	0111	31.41	69.54	33	34.86 227.78	47.49 43.24	81.19 99.49	131.079	2.14					(tq)
86	850824	2153	31.59	66.64	33	273.55 68.39	42.64 50.19	109.06 73.27	170.168	3.871					(tq)
87	850830	0456	33.04	68.65	33	319.08 103.72	20.77 72.81	123.55 78.16	203.08	26.887					(tq)
88	850916	1102	31.95	67.06	33	329.36 137.23	76.35 13.95	92.9 78.22	56.995	31.288					(tq)
89	850930	0212	31.19	69.62	33	117.22 258.95	80.79 11.67	-82.8 -127.69	35.821	53.678					(tq)
90	851204	0443	31.81	67.67	10	208.7 55.8	11.2 80	63.3 95.1	141.5	34.8					(ucr)
91	860811	2206	31.19	67.76	26.5	187	49	167	50	20	0.133	4.9	5.4	5.4	(h)

						285	80	41							
92	880325	1720	31.403	67.989	25	243 1	45 65	143 51	118	11			5.3		(r)
93	990305	0335	34.75	70.25	15	170 12	12 79	69 94	98	34	0.962	5.5	5.2	5.9	(h)
94	011012	0421	33.16	69.04	15	222 314	78 81	171 12	87	2	0.105	5.6	5.1	5.3	(h)
95	020427	2353	31.72	67.78	49.3	341 227	41 71	31 127	291	17	0.0802	4.8	5.3	5.2	(h)
96 *(Event 01074)*	010315	1106	34.82	69.86	3	22.62 188.03	61.41 29.39	97.1 77.22	107.4	16.13	0.0242	4.4	4.8	4.9	*this study*
97 *(Event 01348)*	011214	0117	31.85	67.76	21	23.86 200.78	68.71 21.32	91.12 87.13	113	23.7	0.0145	4.0	5.3	4.7	*this study*
98 *(Event 02074)*	020315	2132	30.908	64.093	21	346.16 207.05	45 52.91	58.52 117.57	277.89	4.22	0.001	2.7	4.7	4.0	*this study*

* the focal mechanism obtained is a composed solution of two events.

(ac) Algermissen et al. (1978)
(a) Assumpção and Araujo (1993)
(c) Chinn and Isacks (1983)
(h) Harvard CMT solutions with centroid epicenter using Dziewonski et al. (1981) method
(i) Inpres (1985)
(k) Kadinsky-Cade (1985)
(r) Regnier et al. (1992); Regnier et al. (1988)
(s) Stauder (1973)
(t -*1979*) Triep (1979)
(t -*1987*) Triep (1987)
(tc) Triep and Cardinali (1984)
(tq) Triep and Quiroga (1989)
(ucr) Universidad de Costa Rica, San José, Costa Rica (from ISC-Bulletin)
(u) USGS online catalog
(v) Volponi (1979)

SEISMIC MOMENT TENSOR ESTIMATION

In this work we present the moment tensor inversion for three shallow earthquakes: one that occurred to the southeast of Sierra Pie de Palo, San Juan (m_b=5.3) on 14 December 2001 (event 01348); another in the eastern flank of the Andes cordillera (south of Mendoza city) (M_D=5.0) on 15 March 2001 (event 01074); and one to the east of Sierra Chica de Córdoba (m_b=4.7) on 15 March 2002 (event 02074) (Figs. 3, 4 and 5).

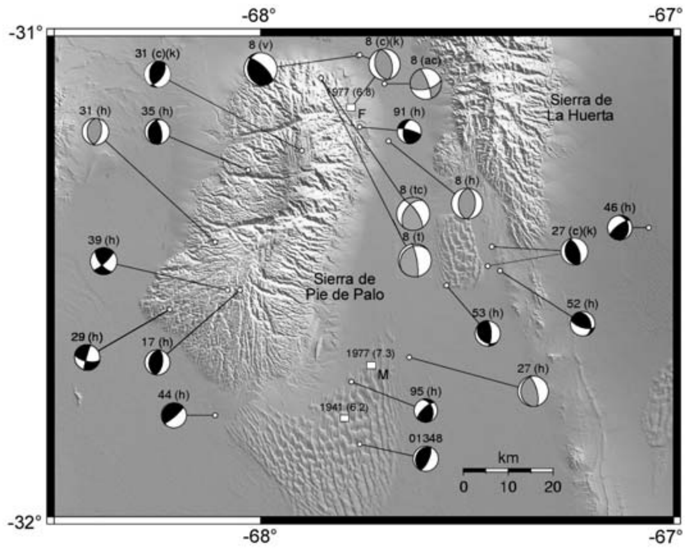

Fig. 5. Same as Fig. 4 showing the seismicity beneath Sierra Pie de Palo and Sierra de Valle Fértil-La Huerta (San Juan, Argentina). The 1977 San Juan earthquake locations for the foreshock (F) and mainshock (M) are from Kadinsky-Cade (1985). The focal mechanism solution for this event (number 6 in Table 1) obtained by Volponi (1979) is shown in black, whereas gray focal mechanism solutions represent different constraints obtained by others authors. Two aftershock determinations (events 25 and 29) are also presented. The focal solution for event 01348 is from this study. (See text and Table 1 for references.)

These were recorded by 22 IRIS-PASSCAL instruments connected to Streckeisen STS-2 (flat velocity response between 0.0083 Hz and 50 Hz) and Guralp CMG-3ESP sensors (velocity response between 0.01 Hz and 50 Hz) (Fig. 1). In addition, we used information recorded by two CMG-40T sensors (velocity response between 0.033 Hz and 50 Hz) from the Instituto Nacional de Prevención Sísmica (INPRES) and Universidad Nacional de San Juan (UNSJ), Argentina (Fig. 1). Location data for the events studied are summarized in Table 1.

The technique used was developed by Randall et al. (1995) and consists of modeling the three-component ground displacements using a layered seismic velocity structure, a fixed hypocentral depth and the calculated Green functions at different event-station distances. In preparing the data for the moment tensor inversion, the instrument response was removed from the vertical, north-south and east-west velocity records to get the corresponding ground displacements. They were rotated into the radial, tangential and vertical components using the epicenter information. An appropriate bandpass filter for the three-displacement component data containing the first P-wave arrival through the surface waves was selected prior to the inversion. We used bandwidth filters in the range 10-50 seconds to reduce the sensitivity of the waveforms to details of the crustal structure and to filter out long-period noise. The signal-to-noise ratio of the observed displacement components was carefully examined in order to eliminate poor quality data. The observed seismograms were fit with synthetic waveforms to determine the double-couple focal mechanism solution, seismic moment, and error of the amplitude misfit. The inversion was repeated for many trial depths to determine the best depth. Thus, a curve showing the amplitude misfit errors versus depth was constructed to estimate the depth of the event that produced the best fit. In most cases, the misfit curve shows a single but sometimes broad minimum. We found that the focal mechanism does not change significantly around the best depth. Moreover, the solution appears insensitive to small perturbations in the seismic velocity model.

In this study, the seismic velocity layered structure used in the inversion was taken from a study of receiver functions that also used

CHARGE data (Shearer, 2002; Shearer et al., 2002). The model is shown in Table 2. In general, the focal mechanism is not very sensitive to the details of the structure, but the depth and waveform fit are sensitive.

We start with seismic event 01348 (m_b=5.3), which occurred to the southeast of Sierra Pie de Palo on 14 December 2001 at GMT time 01:17:53. Accurate waveform modeling depends upon a reliable hypocentral location (errors <5 km). Thus, we located this event by picking P and S wave arrival times recorded on the CHARGE network and then using Hypocenter (Lienert, 1994). We considered the PDE solution (Fig. 3c) as the initial guess to invert for the location parameters. Our final estimation for the epicenter lies 14 km to the southwest of the PDE solution. Interestingly, both global catalogs and our determination indicate a hypocentral depth at 33 km below sea level. Our epicenter location results are shown in Table 1 and Fig. 5.

Table 2. Velocity model (after Shearer, 2002)

Thickness (km)	Vp (km/s)	Vp/Vs	Density (gr/cm^3)
10	5.88	1.70	2.70
35	6.20	1.70	2.85
85*	8.15	1.80	3.30
Halfspace	8.45	1.80	3.30

*mantle velocity gradient

Stations located at epicentral distances between 53 km and 266 km and azimuths between 1º and 301º were used to analyze this earthquake (Fig. 6). Closer stations exhibit relatively larger body waves, whereas surface waves dominate the seismic records for the more distant data. A bandpass filter between 10 and 25 seconds was used before the inversion (Fig. 7). Because all of the data are unweighted during the inversion, closer stations contribute more to the solution. The results of the inversion and all the components used are shown in Figure 8. The residual error versus depth curve shows errors normalized by the sum of the squared amplitudes of the data. Analysis for the depth estimate suggests that it could be in the range of 18-22 km, but the best fit occurs at a depth of 21 km (Fig. 8a). The solution indicates two orthogonal fault planes of strike=23.9º (±0.1º), dip=68.7º (±0.4º) and slip=91.1º (±0.1º) and strike=200.8º (±0º), dip=21.3º (±0.4º) and slip=87.8º (±0.1º), respectively. The errors represent the average difference between the nodal planes for the depth range18-22 km. The seismic moment is M_0=1.45x10^{16} Nm, and the moment magnitude is M_w=4.7.

Although we obtained good fits to the data at most CHARGE stations, there are systematic misfits that could be improved with an improved velocity model. Our future approach will be to fix the focal mechanisms and explore the sensitivity to details of the structure.

Another well-recorded event is earthquake 01074 (M_D=5.0) that occurred on 15 March 2001. Its epicenter is located in the eastern flank of the Cordillera to the south of Mendoza (Fig. 3c). Again, global networks and our determination using Hypocenter located the event at 33 km depth. We also observed that our epicenter solution (34.82ºS, 69.86ºW) is located 33 km to the west of the PDE location (Table 1 and Fig. 4). Using our epicentral determination we tested for the focal depths following a process similar to that described for the previous event. In this case, we considered six stations (mostly with STS2 sensors), located mainly along the south seismic transect at epicentral distances between 108 and 388 km with an azimuth range of 196º. Data were bandpass filtered between 15-50 seconds. Because the vertical displacement observed at the farthest station JUAN showed long-period noise at the beginning of the record, we decided not to include it for the inversion. The moment tensor inversion results and the components used are shown in Figure 9. The residual errors versus depth curve indicates a shallow focal depth in the range 1-5 km with the minimum misfit error at 3 km (Fig. 9a). The focal mechanism solution has two nodal planes with strike=22.6º (±1º), dip=61.4º (±3º) and slip=97.1º (±0º) and strike=188º (±3º), dip=29.4º (±2º) and slip=77.2º (±4º); a seismic moment of M_0=2.42x10^{16} Nm; and a magnitude of M_w=4.9. The errors represent the average difference between the nodal planes for the 1-5 km depth range.

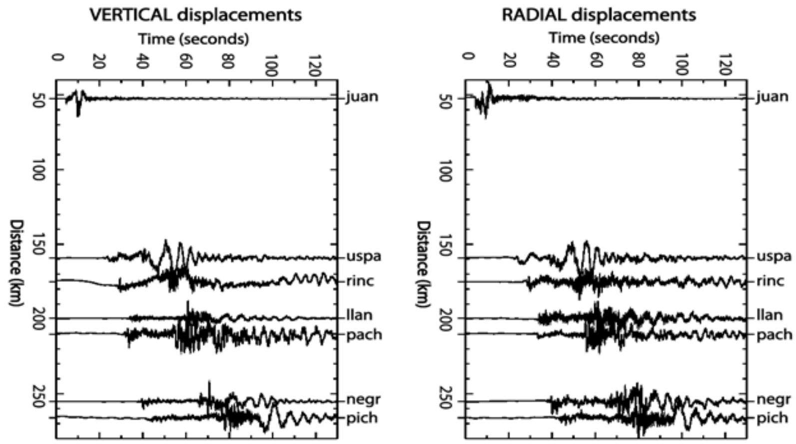

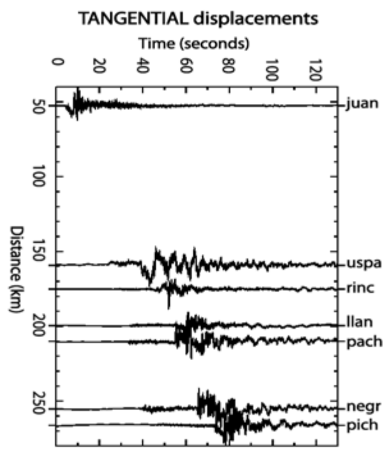

Fig. 6. Record sections showing the vertical, radial and tangential seismic-displacement components at the CHARGE stations (Fig. 1) for event 01348 (m_b=5.3) that occurred on 14 December 2001 to the southeast of the Sierra Pie de Palo, San Juan, Argentina (Fig. 5). Closer stations present relatively higher amplitudes of body waves. Surface waves are more developed at larger epicentral distances. Information from both seismic waves is considered in the seismic moment tensor inversion.

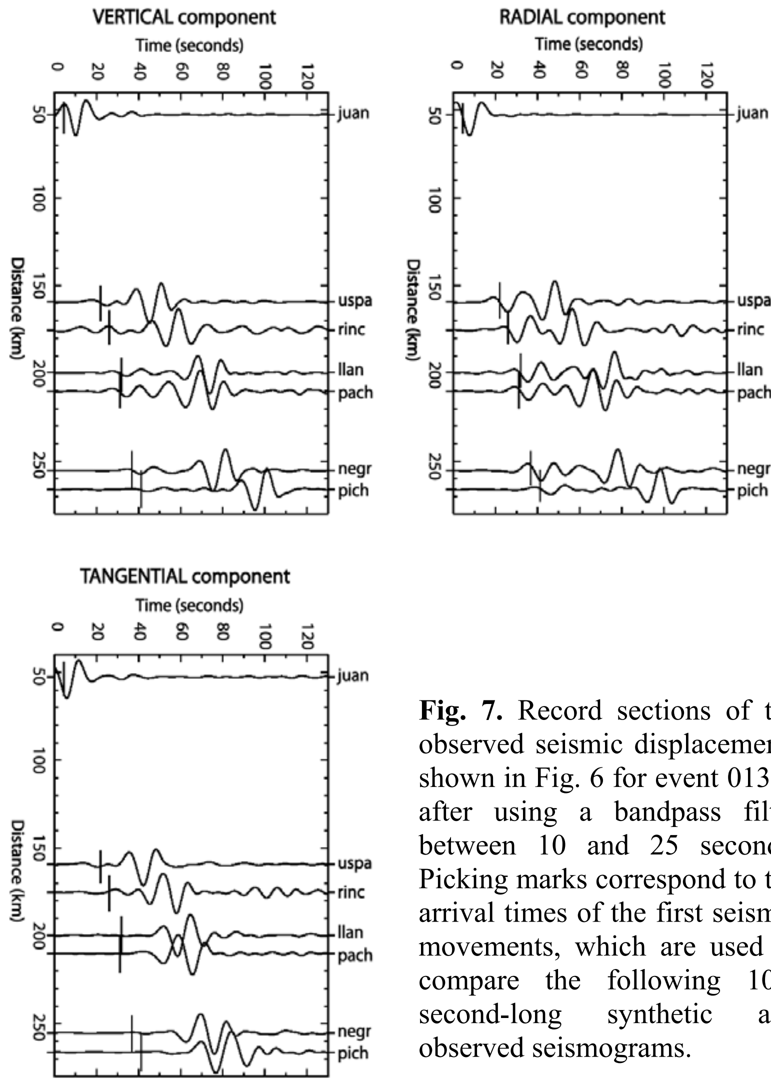

Fig. 7. Record sections of the observed seismic displacements shown in Fig. 6 for event 01348 after using a bandpass filter between 10 and 25 seconds. Picking marks correspond to the arrival times of the first seismic movements, which are used to compare the following 100-second-long synthetic and observed seismograms.

Finally, a smaller event (02074) that occurred on 15 March 2002 at 21:32:28 is analyzed. This earthquake took place in the Eastern Pampean Ranges (Fig. 2 and 3c). We found two difficulties in the analysis of this event: the seismic event is located outside the CHARGE network, and it has a smaller size (m_b=4.7). We modeled this earthquake using the seismic location determined by INPRES (Table 1 and Fig. 4), which is 9 km north of the PDE location. The INPRES depth is 13 km. We were able to use three-component displacements recorded on three seismic stations with STS2 sensors along with several vertical displacements from other stations covering an epicentral distance range between ~100 and 700 km. The azimuthal coverage gap was ~290º. Implications for the inversions with a poor azimuthal coverage result in a greater dependency on the velocity model chosen. A bandwidth of 15-30 seconds was used to filter the data. The moment tensor inversion results for several depths tested show a minimum at 21 km within a possible range between 17-22 km. The nodal planes have strike=346.1º (±7º), dip=45º (±1º) and slip=58.5º (±8º) and strike=207º (±3º), dip=52.9º (±2º) and slip=117.6º (±7º), respectively (Fig. 10). As before the errors represent the average difference between the nodal planes in the depth range of 17-22 km. We also determined a seismic moment of $M_0=1.0x10^{15}$ Nm and a moment magnitude M_w=4.0.

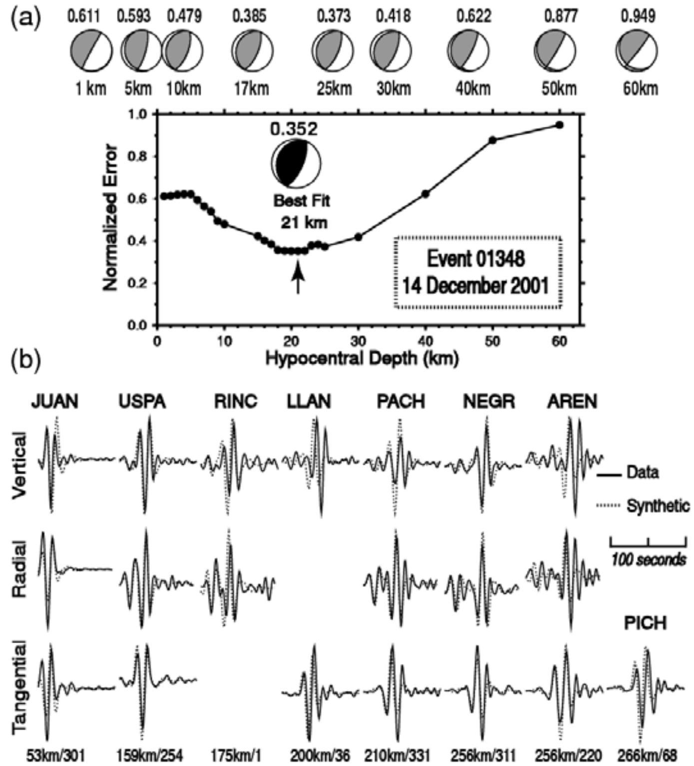

Fig. 8. Results of the seismic moment tensor inversion for event 01348. (a) Hypocentral depths versus the normalized error calculated during the inversion. Black dots on the curve represent each inversion at a fixed depth. Some focal mechanism solutions obtained for them are shown on top with their corresponding error and depth. Note the robustness of the focal mechanism solution for different focal depths. Arrow indicates the depth at which the best data-synthetic fit was achieved (21 km). (b) Solid lines are the observed displacement traces at CHARGE stations (Fig. 6), and dashed lines are the synthetic seismograms for the best-fitting depth (21 km). At the bottom, epicentral distance and azimuth to the station are shown.

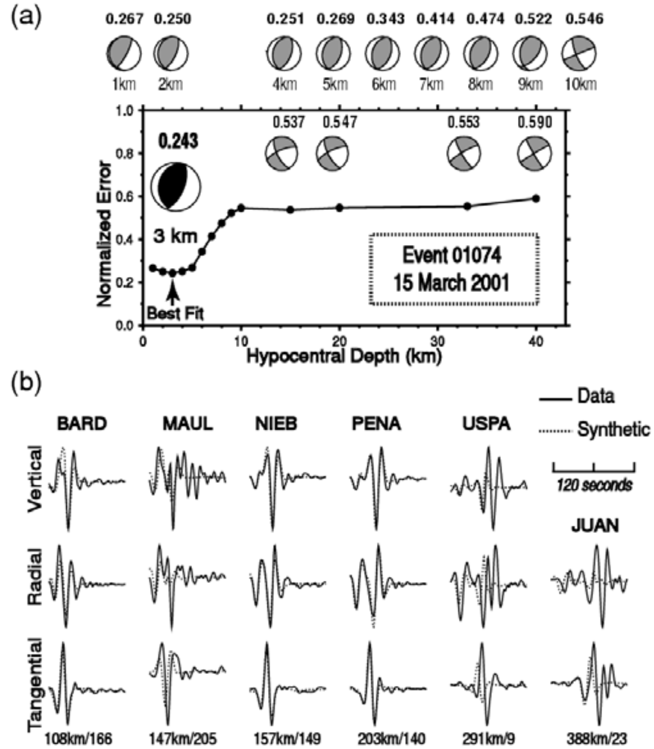

Fig. 9. Results of the seismic moment tensor inversion for event 01074. (a) Curve showing the hypocentral depths tested and the normalized error obtained. The top focal mechanisms show the results for the first 10 km of depth. Again, note the robustness of the focal mechanism solution around the best depth. Arrow indicates the depth at which the best data-synthetic fit was achieved (3 km). (b) Observed displacements (solid lines) at CHARGE stations located at the distances and azimuths indicated at the bottom compared with synthetic seismograms (dashed lines) for the best-fitting depth (3 km). All broadband waveforms were bandpass filtered between 15 and 50 seconds.

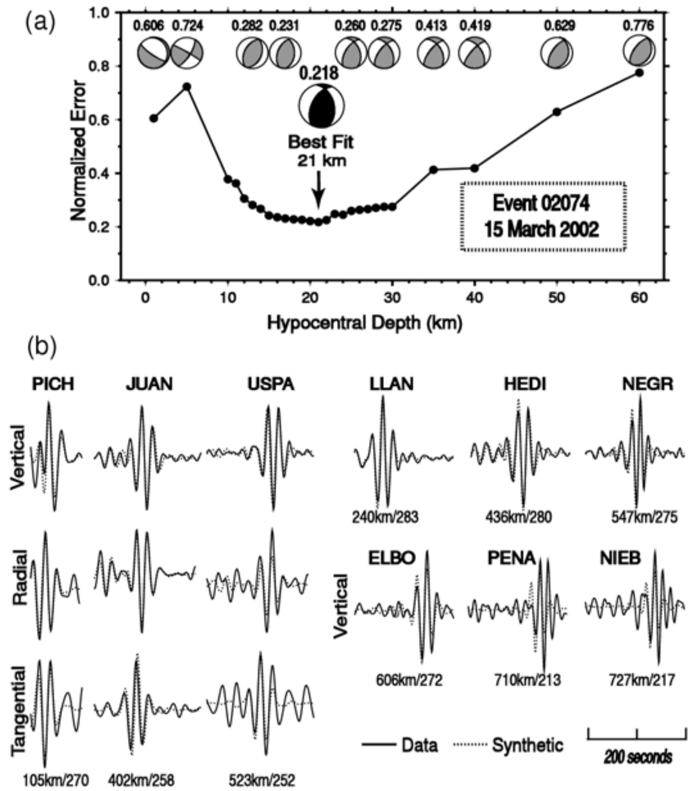

Fig. 10. Results of the seismic moment tensor inversion for the event 02074. (a) Hypocentral depths versus the normalized error calculated for each inversion. Arrow indicates the depth at which the best data-synthetic fit was achieved (21 km). (b) Observed displacements (solid lines) at CHARGE stations located at the distances and azimuths shown at the bottom and synthetic seismograms (dashed lines) for the best fitting depth (21 km). A band-pass filter between 15-30 seconds was used during the inversion.

DISCUSSION AND CONCLUSIONS

We have summarized the crustal seismicity located in the Andean backarc for the past 40 years and have determined focal mechanisms and depths for three crustal earthquakes recorded on a portable broadband seismic network. The three earthquakes located near San Juan, Mendoza, and Córdoba indicate thrust faulting solutions. These observations are in agreement with previous studies and the ~east-west convergence between the Nazca and South American plates. We cannot resolve which of the two nodal planes is the fault plane for these moderate-size earthquakes, but we discuss them in the framework of previous studies for other events that occurred in the region.

Event 01348 is located in the Western Sierras Pampeanas, the best studied region of the Andean backarc because of its high seismic activity. The epicenter is located 14 km south of the 1977 mainshock earthquake (Kadinsky-Cade, 1985) and 6 km south of the INPRES 1941 earthquake location (Fig. 5). The 1977 earthquake was composed of two shocks separated 64 km in a north-south direction and by ~20 seconds. Data from aftershock studies, a short-period seismic experiment, and leveling surveys indicate a system of blind faults dipping to the both east and west directions beneath Sierra Pie de Palo related to this event. According to the interpretation of Regnier et al. (1992), the Sierra Pie de Palo could be divided into two different blocks from north to south. The foreshock and mainshock of 1977 earthquake seem to have their hypocenters in the north and south blocks, respectively. Their local study also revealed a concentration of seismicity in a subhorizontal west-dipping plane and a near-vertical east-dipping plane for the southern block. The earthquake we studied is located in this block as well. Our thrust fault focal mechanism solution agrees with the structure described where either both planes could explain the associated deformation. Two first-motion determinations (events 51 and 52) from Triep and Cardinalli (1984) and one Harvard-CMT determination for the event on 21 August 1978 (event 44) also have similar focal mechanisms (Table 1, Fig. 5).

Event 01074 (Fig. 4) is located near event 93 (Table 1), which occurred previously on 5 March 1999 (M_w=5.9). Figure 4 shows both locations and the focal mechanism solutions which indicate shortening in the Cordillera for the area above a normal-dipping subduction zone. Unlike the north segment, several earthquakes of moderate size are observed in the southern cordillera. On the Chilean side, earthquakes that occurred in Las Melosas (M_s=6.9) in 1958 (Piderit, 1961), and Rancagua (M_s=5.9) in 1987 (Barrientos and Eisenberg, 1988), as well as small-to-moderate size seismicity detected by temporary seismic deployments showed right-lateral strike-slip focal mechanism solutions (Alvarado, 1998; Barrientos et al., 2004). Thus, from the west to the east, it is possible to observe how the deformation in this segment of the Andes responds to local stress state changes. This seismic activity has been observed at levels shallower than 20 km. In particular, our determination shows that the depth of the event on the eastern flank is very shallow (depth < 5 km).

The smallest event successfully modeled (earthquake 02074, M_w=4.0) is located outside the CHARGE network (azimuthal coverage gap of ~290º). The solution indicates that reverse faulting at a depth of 21 km with a small strike-slip component occurs as far as 800 km to the east of the ocean trench. This earthquake is located above the region where the slab begins to descend into the mantle with a more normal subduction angle (Fig. 1). In this region, it is intriguing that no active volcanism is occurring. Volcanic centers related to subduction magmas in this eastern part are in the range ~4.7-7.9 Ma (Gordillo and Linares, 1981; Kay and Gordillo, 1994). On the basis of magnetotelluric studies some thrust faults exposed at the surface and dipping to the east have been interpreted as extending into the base of the crust (~50km depth) rather than becoming listric (Booker et al., 2002). Considering these observations, our results reveal that the plane oriented N-NW dipping 45º to the east is the most likely active fault plane related to this earthquake. It also represents the first focal mechanism determination in the Eastern Pampean Ranges confirming how far the Andean deformation penetrates into cratonic South America.

The backarc of the South Central Andes in Argentina continues to be in compression and results in thrust earthquakes through out much of the crust. The intense crustal seismic activity extends to the central part of the country and evidences a cold crust. The addition of broadband seismic stations makes possible to determine both focal mechanisms and depths of small-to-moderate earthquakes. This seismicity is more abundant and can give us good constraints to discuss the tectonics of the region.

(*) Terry Wallace (UofA), Keith Kopper (Saint Luis University), Robert Fromm (UofA), Lara Wagner (UofA), Todd Shearer (UofA), Megan Anderson (UofA), Hersh Gilbert (UofA), Mario Bufaliza (INPRES), Norberto Puebla (INPRES), Oscar Marcuzzi (INPRES), Rolando Vila (INPRES), Miguel Gaitán (INPRES), Jaime Campos (Universidad de Chile-UCH), Edgar Kausel (UCH), Javier Ruiz (UCH), Roxana Dominguez (UNSJ), Mariana Aguiar (Repsol-YPF), Gabriela Bustos (UNSJ), Federico Lince-Klinger (UNSJ), Martín Mallea (UNSJ), Paulo López (UNSJ), Cintia Ponce (UNSJ), Juan Carlos Rodriguez (UNSJ), and Patricia Torés (UNSJ).

Acknowledgments: National Science Foundation grant EAR-9811878 supported the project CHARGE (www.geo.arizona.edu/CHARGE). The instruments used in the field program were provided by the PASSCAL facility of the Incorporated Research Institutions for Seismology (IRIS) through the PASSCAL Instrument Center at New Mexico Tech. Data collected during this experiment will be available through the IRIS Data Management Center. The facilities of the IRIS Consortium are supported by the National Science Foundation under Cooperative Agreement EAR-0004370. Processing of the seismic data was performed using Seismic Analysis Code SAC2000 software (Goldstein et al., 1999). Maps were generated using Graphic Mapping Tools software. We also used seismological data retrieved from the International Seismological Centre, and Harvard-CMT on-line Bulletins.

We would like to thank Miss María Inés López from the Secretaría de Ciencia y Técnica de Rectorado, Departamento de Geofísica y Astronomía, and Facultad de Ciencias Exactas, Físicas y Naturales from the Universidad Nacional de San Juan (Argentina); Instituto Nacional de Prevención Sísmica (Argentina); and Departamento de Geofísica, Universidad de Chile (Chile) for their scientific and logistical support.

We are very grateful for the valuable help during the field work in Argentina from Ministerio de Obras y Servicios Públicos, San Juan Government; Escuadrón 25 "Jáchal" (San Juan) and Escuadrón 29 "Malargüe" (Mendoza) from Gendarmería Nacional; Embalse Las Pichanas and familia Farroni, DIPAS-Repartición Cruz del Eje (Córdoba); Parque Nacional Ischigualasto-Valle de la Luna (Ischigualasto, San Juan); Dique Nivelador Pachimoco (San Juan); Municipalidad and Secretaría de Turismo de Malargüe (Mendoza), Puesto "Los Rincones" (familia Ontiveros, Ischigualasto, San Juan); "Puesto Las Peñas" (familia Pérez, Malargüe, Mendoza), "Puesto Vega-Miranda" (familia Miranda, Malargüe, Mendoza), "Puesto La Niebla" (familia Zambrano, Malargüe, Mendoza).

Mario Pardo, Armando Imhof, and Miguel Pérez helped us to obtain useful seismological information. We thank Mauro Saez for his computer assistance in the preparation of this paper.

REFERENCES

Algermissen S., J.C. Castano, C. Langer, S. Harding, R. Bucknan and E. Uliarte, A preliminary report on the western Argentina earthquake of November 23, 1977. *Earthquake Notes, 49*, N^o 1, p. 40, 1978.

Allmendinger R., D. Figueroa, E. Synder, J. Beer, C. Mpodozis and B.L. Isacks, Foreland shortening and crustal balancing in the Andes at 30ºS latitude. *Tectonics, 9*, 789-809, 1990.

Alvarado P.M., Sismicidad superficial de los Andes Centrales (33º-35ºS; 69.5º-70.5ºW). *Tesis de Magister en Ciencias, mención Geofísica*. Facultad de Ciencias Físicas y Matemáticas, Universidad de Chile. 161 pp, 1998.

Assumpção M., The regional intraplate stress field in South America. *J. Geophys. Res., 97*, 11889 – 11903, 1992.

Assumpção M. and M. Araujo, Effect of the Altiplano-Puna plateau, South America, on the regional intraplate stresses. *Tectonophysics, 221*, 475-496, 1993.

Baldis B., M.S. Beresi, O. Bordonaro and A. Vaca, Síntesis evolutiva de la Precordillera Argentina. *V Congreso Latinoamericano de Geología Argentina, Actas, vol. 1*, 399-445, Buenos Aires, 1982.

Barrientos S., E. Vera, P. Alvarado and T. Monfret, Crustal seismicity in Central Chile. Accepted for publication in *J. S. Am. Earth Sci.,* 2004.

Barrientos S. and A. Eisenberg, Secuencia sísmica en la zona cordillerana al interior de Rancagua. *V Congreso Geológico Chileno, Santiago*, F121-F132, 1988.

Bastías H., N. Weidmann and M. Pérez, Dos zonas de fallamiento pliocuaternaria en la Precordillera de San Juan. *IX Congreso Geológico Argentino, Tomo II, Actas II*, 329-341, 1984.

Booker J., M.C. Pomposiello, A. Favetto, B. Narod and G. Giordanengo, Electrical conductivity structure beneath Córdoba province, Argentina. *Actas del XV Congreso Geológico Argentino*, CD-Rom, 2002.

Cahill T. and B. Isacks, Seismicity and shape of the subducted Nazca plate. *J. Geophys. Res., 97*, 17503 – 17529, 1992.

Caminos R., Sierras Pampeanas noroccidentales, Salta, Tucumán, Catamarca, La Rioja y San Juan. *Segundo Simposio de Geología Regional Argentina: Córdoba, Acad. Nac. Cienc., 1*, 225-292, 1979.

Castellanos A., Contribución a los estudios sísmicos en la República Argentina. El caso de San Juan. *Monografías, Universidad Nacional del Litoral, Rosario Argentina, Tomos I, II, III*, 1944.

Chiaramonte L., V.A. Ramos and M. Araujo, Estructura y sismotectónica del anticlinal Barrancas, cuenca Cuyana, provincia de Mendoza. *Revista de la Asociación Geológica Argentina, 55*, 309-336, 2000.

Chinn D.S. and B.L. Isacks, Accurate source depths and focal mechanisms of shallow earthquakes in western South America and New Hebrides Island Arc. *Tectonics, 2,* 529-563, 1983.

Costa C.H. and Vita-Finzi C., Late Holocene faulting in the southeast Sierras Pampeanas of Argentina. *Geology, 24*, 1127-1130, 1996.

Cristallini E.O and V.A. Ramos, Thick-skinned and thin-skinned thrusting in La Ramada fold-and-thrust belt. Crustal evolution of the High Andes of San Juan, Argentina (32°SL). *Tectonophysics, 317,* 205-235, 2000.

DeMets C., R.G. Gordon, D.F. Argus and S. Stein, Current plate motions. *Geophys. J. Int., 101,* 425-478, 1990.

Dziewonski A.M., T.A. Chou and J.H. Woodhouse, Determination of earthquake source parameters from waveform data for studies of global and regional seismicity. *J. Geophys. Res., 86,* 2825-2852, 1981.

Ganse R.A. and J.B. Nelson, Catalog of significant earthquakes 2000 B.C.-1979 including quantitative casualties and damage. *World Data Center A for Solid Earth Geophysics, Report SE-27*. Boulder, Colorado, USA, 1981.

Goldstein P., D. Dodge and M. Firpo, SAC2000: Signal processing and analysis tools for seismologists and engineers, UCRL-JC-135963. Invited contribution to the IASPEI International Handbook of Earthquake and Engineering Seismology, 1999.

Gordillo C.E. and A. Linares, Geocronología y petrografía de las vulcanistas terciarias del Departamento de Pocho, Provincia de Córdoba. *Revista de la Asociación Geológica Argentina, 36*, 380-388, 1981.

Groeber R.P., Movimientos tectónicos contemporáneos y un nuevo tipo de dislocaciones. *Notas del Museo de La Plata. Tomo IX*, 1944.

Gutscher, M., W. Spakman, H. Bijwaard, and R. Enghdal, Geodynamics of flat subduction: Seismicity and tomographic constraints from the Andean Margin. *Tectonics*, *19,* 814-833, 2000.

INPRES, El terremoto de Mendoza Argentina del 26 de enero de 1985 - Informe General. *Instituto Nacional de Prevención Sísmica INPRES - República Argentina*, 1985.

INPRES, Listado de sismos históricos de Argentina (www.inpres.gov.ar), 2003.

Jordan T.E. and R.W. Allmendinger, The Sierras Pampeanas of Argentina: A modern analogue of Rocky Mountain foreland deformation. *American Journal of Science, 286*, 737-764, 1986.

Kadinsky-Cade K., Seismotectonic of the Chilean margin and the 1977 Caucete earthquake of western Argentina. *Ph.D. Thesis,* Cornell University, Ithaca, New York, 253 pp, 1985.

Kadinsky-Cade K., R. Reilinger and B. Isacks, Surface deformation associated with the November 23, 1977, Caucete, Argentina, earthquake sequence. *J. Geophys. Res., 90*, 12691-12700, 1985.

Kay S.M. and C.E. Gordillo, Pocho volcanic rocks and the melting of depleted continental lithosphere above a shallowly dipping subduction zone in the central Andes. *Contribution to Mineralogy and Petrology, 117*, 25-44, 1994.

Kay S.M., V. Maksaev, R. Moscoso, C. Mpodozis, C. Nasi and C.E. Gordillo, Tertiary magmatism in Chile and Argentina between 28ºS and 33ºS: Correlation of magmatic chemistry with changing Benioff zone. *J. S. Am. Earth Sci., 1*, 21-38, 1988.

Kay S.M. and C. Mpodozis, Magmatism as a probe to the Neogene shallowing of the Nazca plate beneath the modern Chilean flat slab. *J. S. Am. Earth Sci., 15*, 39-57, 2002.

Langer C.J. and G.A. Bollinger, Aftershocks of the western Argentina (Caucete) earthquake of 23 November 1977: some tectonic implications. *Tectonophysics, 148*, 131-146, 1988.

Lienert B.R., Users manual for HYPOCENTER 3.2: A computer program for locating earthquakes locally, regionally and globally. *Hawaii Inst. of Geophys. and Planetology. Publ. 1-72*, 1994.

Mc Donough M.R., V.A. Ramos, C.E. Isachsen, S.A. Bowring and G.I. Vujovich, Edades preliminares de circones del basamento de la Sierra de Pie de Palo, Sierras Pampeanas Occidentales de San Juan: Sus implicancias para el supercontinente Proterozoico de Rodinia. *XII Congreso Geológico Argentino, Actas 3*, 340-342, 1993.

Nábelek J., Determination of earthquake source parameters from inversion of body waves. *Ph.D. Thesis,* Massachusetts Institute of Technology, Cambridge, Mass, USA, 1984.

Peruca L. and J.D. Paredes, Fallamiento cuaternario en la zona de La Laja y su relación con el terremoto de 1944, Departamento Albardón, San Juan, Argentina. *Revista Mexicana de Ciencias Geológicas, 20*, 20-26, 2003.

Piderit E., Estudio de los sismos del Cajón del Maipo del año 1958. *Memoria para optar al título de Ingeniero Civil.* Facultad de Ciencias Físicas y Matemáticas, Universidad de Chile, 125 pp, 1961.

Ramos V.A., The tectonics of the Central Andes: 30º to 33ºS latitude. In Processes in continental lithospheric deformation. Clark S., Burchfiel D. (Eds.) *Geological Society of America. Paper 218*, 31-54, 1988.

Ramos V., Foothills structure in the Northern Magallanes Basin, Argentine. *AAPG Bulletin 73*, 887-903 1989.

Ramos V., F. Munizaga and S. Kay, El magmatismo cenozoico a los 33º de latitud: geocronologia y relaciones tectonicas. *VI Congreso Geológico Chileno, Actas I*, 892-896, 1991.

Ramos V.A., M. Cegarra and E. Cristallini, Cenozoic tectonics of the High Andes of west-central Argentina (30-36º S latitude). *Tectonophysics, 259*, 185-200, 1996.

Ramos V.A., E.O. Cristallini and D.J. Pérez, The Pampean flat-slab of the central Andes. *J. S. Am. Earth Sci., 15*, 59-78, 2002.

Randall G.E., C.J. Ammon and T.J. Owens, Moment-tensor estimation using regional seismograms from a Tibetan Plateau portable network deployment. *Geophys. Res. Letters, 22*, 1665-1668, 1995.

Regnier M., J.L. Chatelain, R. Smalley (Jr.), J.M. Chiu, B. Isacks and M. Araujo, Seismotectonics of Sierra Pie de Palo, a basement block upflit in the Andean foreland of Argentina. *Bull. Seism. Soc. Am., 82,* 2549-2571, 1992.

Regnier M., R. Smalley (Jr.), J.M. Chiu, D. Vlasity, J. Pujol, A.C. Johnston, G.C. Steiner, J. Bollwerk, J. Vlasity, B.L. Isacks, T. Cahill, D. Whitman, J.L. Chatelain, F. Bondoux, J.C. Castano and N. Puebla, Analysis of an Mb 5.3 earthquake and its aftershock sequence in the thick-skinned Sierras Pampeanas of the Andean Foreland. *EOS, 69,* No. 44, 1988.

Shearer M.T., Crust and upper mantle structure of the Sierras Pampeanas, south-central Andes. *M.Sc. Thesis,* University of Arizona, 2002.

Shearer T., S. Beck, G. Zandt, P. Alvarado, E. Triep, M. Araujo, M. Bufaliza and J. Campos, Lithospheric structure of the Sierras Pampeanas, South Central Andes. *American Geophysical Union, Fall meeting abstracts*, San Francisco, 2002.

Smalley R.(Jr.), J. Pujol, M. Regnier, J.M. Chiu, J.L. Chatelain, B.L. Isacks, M. Araujo and N. Puebla, Basement seismicity beneath the Andean Precordillera thin-skinned thrust belt and implications for crustal and lithospheric behavior. *Tectonics, 12*, 63-76, 1993.

Snyder D.B., V.A. Ramos and R.W. Allmendinger, Thick-skinned deformation observed on deep seismic reflection profiles in western Argentina. *Tectonics, 9*, 773-788, 1990.

Stauder W., Mechanism and spatial distribution of Chilean earthquakes with relation to subduction of the oceanic plate. *J. Geophys. Res., 78,* 5033-5061, 1973.

Triep E.G., Source mechanism of San Juan Province earthquake, 1977. *International Institute of Seismology and Earthquake Engineering (Japan), Individual Studies, Vol. 15*, pp. 1-14, 1979.

Triep E.G., La falla activada durante el sismo principal de Mendoza de 1985 e implicaciones tectónicas. *X Congreso Geológico Argentino, Actas 1*, 199-202, 1987.

Triep E.G. and C.B. de Cardinalli, Mecanismos de sismos en las Sierras Pampeanas Occidentales. *IX Congreso Geológico Argentino, Actas 3*, 61-80, 1984.

Triep E.G. and M. Quiroga, Análisis sismotectónico de mecanismos focales en regiones del retroarco andino, San Juan. *Universidad Nacional de San Juan, Instituto Sismológico Zonda,* 120 pp, Argentina, 1989.

Volponi F.S., M. Quiroga and A.J. Mendiguren, Movimientos actuales en la superficie de la corteza terrestre (Estudio del sismo del 24 de diciembre de 1964). In *Anales de la Sociedad Científica Argentina, Tomo 181*, Entregas I-II, 11-20, Buenos Aires, 1966.

Volponi F.S., Report of the Argentina-United States binational symposium about Caucete earthquake of November 23rd, 1977. *Universidad Nacional de San Juan, Instituto Sismológico Zonda, San Juan, Argentina,* 44 pp, 1979.

Yañez G.A., J. Cembrano, M. Pardo, C. Ranero and D. Selles, The Challenger-Juan Fernández-Maipo major tectonic transition of the Nazca-Andean subduction system at 33-34ºS: Geodynamic evidence and implications. *J. S. Am. Earth Sci., 15*, 23-38, 2002.

Zamarbide J.L. and J.C. Castano, Analysis of the January 26th, 1985, Mendoza (Argentina) earthquake effects and of their possible correlation with the recorded accelerograms and soil conditions. *Tectonophysics, 218*, 221-235, 1993.

Zapata T.R., Crustal structure of the Andean thrust front at 30ºS latitude from shallow and deep seismic reflection profiles, Argentina. *J. S. Am. Earth Sci., 11*, 131-151, 1998.

Zapata T.R. and R.W. Allmendinger, Thrust-front zone of the Precordillera, Argentina: A thick-skinned triangle zone. *AAPG Bulletin, 3*, 359 – 381, 1996.